angiogenesis.

Carbonated springs have been used as spa therapy for many years to treat a variety of diseases, particularly in European countries. It is also well known that CO_2-enriched water induces peripheral vasodilatation, which increases the cutaneous blood flow[14, 15]. Furthermore, Toriyama *et al.* reported that the effects of CO_2-enriched water on the subcutaneous microcirculation are mediated by peripheral vasodilation resulting from increased parasympathetic and decreased sympathetic nerve activity[16]. Furthermore, a recent study showed that the immersion of ischemic hindlimbs into CO_2-enriched water results in a NO-dependent increase in collateral blood perfusion in mice in a unilateral hindlimb ischemia model[9]. Hence, highly concentrated CO_2 is thought to be useful for treating ischemic diseases. However, devising an artificial CO_2-rich bath system is difficult.

Although carbonated spring water has been found to contain more than 1,000 ppm of CO_2, it is difficult to constantly maintain the CO_2 concentration above 1,000 ppm for hours. In contrast, CO_2 dry mist production units can easily produce CO_2 concentrations of more than 900,000 ppm[10]. In the present study, we assessed whether treatment with CO_2 mist exerts an angiogenic effect in rodent ischemic hindlimbs and investigated the mechanisms responsible for the proangiogenic effects induced by CO_2 mist. The main finding of the present study is that percutaneously administered CO_2 mist accelerates angiogenesis, compared with no treatment or treatment with CO_2 gas or air mist, in mice with hindlimb ischemia.

There are several possible mechanisms for the effects of CO_2 mist. For example, the transfer of CO_2 across the skin results in beneficial local vasomotor effects without inducing systemic hemodynamic modifications[8]. In the present study, treatment with CO_2 mist, but not gas, had vasodilatory effects in rat femoral subcutaneous tissue (**Fig. 1-E** to **H**). These results suggest that CO_2 mist exerts a vasodepressor effect. Furthermore, the CO_2 mist significantly increased the oxy-Hb levels and significantly decreased the deoxy-Hb levels compared with the CO_2 gas (**Fig. 1-I** and **J**). Interestingly, the StO_2 levels were also significantly higher in the CO_2 mist group than in the CO_2 gas group (**Fig. 1-L**). These findings suggest that CO_2 mist increases the blood flow, consequently shortening the blood capillary transit time, thereby reducing the process of extraction of oxygen from the blood and releasing oxygen more easily.

A recent study demonstrated that the expression levels of potent angiogenic factors, such as VEGF or FGF-2, are increased and endothelial cell apoptosis is inhibited in endothelial cells cultured in medium equilibrated with hypercapnia-associated acidosis[17]. It has also been established that VEGF promotes ischemia-induced angiogenesis[18-20]. The present data further indicate that the VEGF and FGF-2 expression is induced in the hindlimb skeletal muscles by CO_2 mist treatment (**Fig. 3**), while the VEGF protein level is increased by CO_2 mist (**Fig. 4**). The increase in the VEGF expression caused by CO_2 mist treatment may, at least partially, contribute to angiogenesis after ischemia. Interestingly, treatment with CO_2 gas, as well as mist, significantly increased the VEGF expression on day 14 only in the present study, suggesting that CO_2 gas alone may increase the VEGF expression in the chronic phase, although the effect may not be intense.

Previous studies have reported that VEGF stimulates the release of NO from the arterial wall[21] and promotes the recovery of a disturbed endothelium-dependent flow in the ischemic hindlimb. Moreover, the involvement of NO in the angiogenic effects of VEGF has been established in NO-deficient mice[19, 22]. In the current analysis, CO_2 mist treatment significantly increased the eNOS mRNA activity, but not its expression (**Fig. 4**), as well as the serum NO_3^- concentration compared with that observed without treatment or treatment with CO_2 gas or air mist (**Fig. 5-A**). Furthermore, the inhibition of the NOS activity by L-NAME completely inhibited the recovery of the collateral blood flow induced by the CO_2 mist (**Fig. 5-B**). Furthermore, the CO_2 mist significantly increased the LDBF ratio in the $iNOS^{-/-}$ mice, but not in the $eNOS^{-/-}$ mice (**Fig. 5-C** and **D**). Taken together, these findings demonstrate that the proangiogenic effects of CO^2 mist are the product of the activation of eNOS-mediated signaling resulting from the downstream effects of VEGF. Very interestingly, treatment with CO_2 mist using highly concentrated CO_2 (100% CO_2 gas) significantly accelerated the blood flow recovery in the ischemic hindlimbs. In contrast, treatment with CO_2 mist using a low concentration of CO_2 only slightly recovered the blood flow in the ischemic hindlimbs (**Fig. 6**). These results suggest that blood flow recovery may be enhanced in a CO_2 concentration-dependent manner.

In order to further investigate the mechanisms underlying the effects of CO_2 mist, we performed a proteomic analysis of the hindlimb muscles four days after ischemia. Interestingly, the levels of 18 of 68 proteins upregulated by ischemia were decreased by CO_2 mist treatment. Rap1, a small GTPase, has been shown to regulate multiple basic cellular processes, and there is emerging evidence that Rap1 regulates basic endothelial responses to angiogenic stimulation[23, 24]. In the

present study, the Rap1b level was remarkably increased by ischemia and subsequently decreased by treatment with CO_2 mist. Therefore, CO_2 mist may regulate excessive Rap1 and ERK activation in the hindlimb muscles, although there are currently no reports concerning the role of Rap1 in skeletal muscle.

On the other hand, we found that, of the 62 proteins downregulated by ischemia, the levels of 21 proteins were increased by CO_2 mist treatment. Some of these proteins are enzyme proteins involved in the glycolytic system, such as GAPDH, glucose phosphate isomerase 1, enolase and aldolase A. Therefore, CO_2 mist treatment may promote metabolism in ischemic muscles. Oxidative stress occurs when the production of reactive oxygen species (ROS) is enhanced and/or the antioxidant reserve is suppressed. Enhanced ROS production decreases the bioavailability of NO via an oxidative reaction that inactivates NO[25]. Signal *et al.* provided evidence of a progressive decrease in the SOD and catalase activity in an infarcted rat heart[26]. In addition, the present data show that the SOD2 level is decreased by ischemia and increased by CO_2 mist treatment. Therefore, CO_2 mist may have antioxidant actions.

Study Limitations

The proteomic analysis identified novel protein candidates regulated by the CO_2 mist. However, it could not be determined which molecules are directly regulated by CO_2 mist. Therefore, further studies are needed to explore the precise mechanisms underlying CO_2 mist-induced angiogenesis.

In conclusion, this study provides the first evidence that CO_2 mist promotes angiogenesis after ischemia, at least partially, by increasing the subcutaneous blood flow, as well as the VEGF and NO levels, in ischemic muscles. Hence, CO_2 mist therapy is potentially useful for treating patients with PAD.

Acknowledgments

The authors thank Ms. Chiori Asahi and Ms. Azusa Inagaki for their technical assistance. This study was supported in part by Advance Biotron Co., Ltd., Tokyo, Japan.

COI

The authors have no conflicts of interest to declare.

References

1) Garg PK, Liu K, Tian L, Guralnik JM, Ferrucci L, Criqui MH, Tan J, McDermott MM: Physical activity during daily life and functional decline in peripheral arterial disease. Circulation, 2009; 119: 251-260
2) McDermott MM, Liu K, Greenland P, Guralnik JM, Criqui MH, Chan C, Pearce WH, Schneider JR, Ferrucci L, Celic L, Taylor LM, Vonesh E, Martin GJ, Clark E: Functional decline in peripheral arterial disease: associations with the ankle brachial index and leg symptoms. JAMA, 2004; 292: 453-461
3) Berger JS, Hiatt WR: Medical therapy in peripheral artery disease. Circulation, 2012; 126: 491-500
4) Hiatt WR: Medical treatment of peripheral arterial disease and claudication. N Engl J Med, 2001; 344: 1608-1621
5) Hirsch AT, Haskal ZJ, Hertzer NR, Bakal CW, Creager MA, Halperin JL, Hiratzka LF, Murphy WR, Olin JW, Puschett JB, Rosenfield KA, Sacks D, Stanley JC, Taylor LM Jr, White CJ, White J, White RA: ACC/AHA 2005 Practice Guidelines for the management of patients with peripheral arterial disease (lower extremity, renal, mesenteric, and abdominal aortic): a collaborative report from the American Association for Vascular Surgery/Society for Vascular Surgery, Society for Cardiovascular Angiography and Interventions, Society for Vascular Medicine and Biology, Society of Interventional Radiology, and the ACC/AHA Task Force on Practice Guidelines (Writing Committee to Develop Guidelines for the Management of Patients With Peripheral Arterial Disease): endorsed by the American Association of Cardiovascular and Pulmonary Rehabilitation; National Heart, Lung, and Blood Institute; Society for Vascular Nursing; TransAtlantic Inter-Society Consensus; and Vascular Disease Foundation. Circulation, 2006; 113: e463-654
6) Miyauchi T, Miyata M, Ikeda Y, Akasaki Y, Hamada N, Shirasawa T, Furusho Y, Tei C: Waon therapy upregulates Hsp90 and leads to angiogenesis through the Akt-endothelial nitric oxide synthase pathway in mouse hindlimb ischemia. Circ J, 2012; 76: 1712-1721
7) Rokutanda T, Izumiya Y, Miura M, Fukuda S, Shimada K, Izumi Y, Nakamura Y, Araki S, Hanatani S, Matsubara J, Nakamura T, Kataoka K, Yasuda O, Kaikita K, Sugiyama S, Kim-Mitsuyama S, Yoshikawa J, Fujita M, Yoshiyama M, Ogawa H: Passive exercise using whole-body periodic acceleration enhances blood supply to ischemic hindlimb. Arterioscler Thromb Vasc Biol, 2011; 31: 2872-2880
8) Savin E, Bailliart O, Bonnin P, Bedu M, Cheynel J, Coudert J, Martineaud JP: Vasomotor effects of transcutaneous CO2 in stage II peripheral occlusive arterial disease. Angiology, 1995; 46: 785-791
9) Irie H, Tatsumi T, Takamiya M, Zen K, Takahashi T, Azuma A, Tateishi K, Nomura T, Hayashi H, Nakajima N, Okigaki M, Matsubara H: Carbon dioxide-rich water bathing enhances collateral blood flow in ischemic hindlimb via mobilization of endothelial progenitor cells and activation of NO-cGMP system. Circulation, 2005; 111: 1523-1529
10) Yamazaki T, Izumi Y, Nakamura Y, Hanatani A, Shimada K, Muro T, Shiota M, Iwao H, Yoshiyama M: Novel

device that produces carbon dioxide mist for myocardial infarction treatment in rats. Circ J, 2012; 76: 1203-1212
11) Izumi Y, Shiota M, Kusakabe H, Hikita Y, Nakao T, Nakamura Y, Muro T, Miura K, Yoshiyama M, Iwao H: Pravastatin accelerates ischemia-induced angiogenesis through AMP-activated protein kinase. Hypertens Res, 2009; 32: 675-679
12) Shiota M, Kusakabe H, Izumi Y, Hikita Y, Nakao T, Funae Y, Miura K, Iwao H: Heat shock cognate protein 70 is essential for Akt signaling in endothelial function. Arterioscler Thromb Vasc Biol, 2010; 30: 491-497
13) Takahashi K, Tanaka M, Inagaki A, Wanibuchi H, Izumi Y, Miura K, Nagayama K, Shiota M, Iwao H: Establishment of a 5-fluorouracil-resistant triple-negative breast cancer cell line. Int J Oncol, 2013; 43: 1985-1991
14) Hartmann BR, Bassenge E, Pittler M: Effect of carbon dioxide-enriched water and fresh water on the cutaneous microcirculation and oxygen tension in the skin of the foot. Angiology, 1997; 48: 337-343
15) Ito T, Moore JI, Koss MC: Topical application of CO2 increases skin blood flow. J Invest Dermatol, 1989; 93: 259-262
16) Toriyama T, Kumada Y, Matsubara T, Murata A, Ogino A, Hayashi H, Nakashima H, Takahashi H, Matsuo H, Kawahara H: Effect of artificial carbon dioxide foot bathing on critical limb ischemia (Fontaine IV) in peripheral arterial disease patients. Int Angiol, 2002; 21: 367-373
17) D'Arcangelo D, Facchiano F, Barlucchi LM, Melillo G, Illi B, Testolin L, Gaetano C, Capogrossi MC: Acidosis inhibits endothelial cell apoptosis and function and induces basic fibroblast growth factor and vascular endothelial growth factor expression. Circ Res, 2000; 86: 312-318
18) Izumi Y, Kim-Mitsuyama S, Yoshiyama M, Omura T, Shiota M, Matsuzawa A, Yukimura T, Murohara T, Takeya M, Ichijo H, Yoshikawa J, Iwao H: Important role of apoptosis signal-regulating kinase 1 in ischemia-induced angiogenesis. Arterioscler Thromb Vasc Biol, 2005; 25: 1877-1883
19) Murohara T, Asahara T, Silver M, Bauters C, Masuda H, Kalka C, Kearney M, Chen D, Symes JF, Fishman MC, Huang PL, Isner JM: Nitric oxide synthase modulates angiogenesis in response to tissue ischemia. J Clin Invest, 1998; 101: 2567-2578
20) Namba T, Koike H, Murakami K, Aoki M, Makino H, Hashiya N, Ogihara T, Kaneda Y, Kohno M, Morishita R: Angiogenesis induced by endothelial nitric oxide synthase gene through vascular endothelial growth factor expression in a rat hindlimb ischemia model. Circulation, 2003; 108: 2250-2257
21) van der Zee R, Murohara T, Luo Z, Zollmann F, Passeri J, Lekutat C, Isner JM: Vascular endothelial growth factor/vascular permeability factor augments nitric oxide release from quiescent rabbit and human vascular endothelium. Circulation, 1997; 95: 1030-1037
22) Aicher A, Heeschen C, Mildner-Rihm C, Urbich C, Ihling C, Technau-Ihling K, Zeiher AM and Dimmeler S: Essential role of endothelial nitric oxide synthase for mobilization of stem and progenitor cells. Nat Med, 2003; 9: 1370-1376
23) Carmona G, Gottig S, Orlandi A, Scheele J, Bauerle T, Jugold M, Kiessling F, Henschler R, Zeiher AM, Dimmeler S, Chavakis E: Role of the small GTPase Rap1 for integrin activity regulation in endothelial cells and angiogenesis. Blood, 2009; 113: 488-497
24) Chrzanowska-Wodnicka M: Regulation of angiogenesis by a small GTPase Rap1. Vascul Pharmacol, 2010; 53: 1-10
25) Droge W: Free radicals in the physiological control of cell function. Physiol Rev, 2002; 82: 47-95
26) Hill MF, Singal PK: Right and left myocardial antioxidant responses during heart failure subsequent to myocardial infarction. Circulation, 1997; 96: 2414-2420

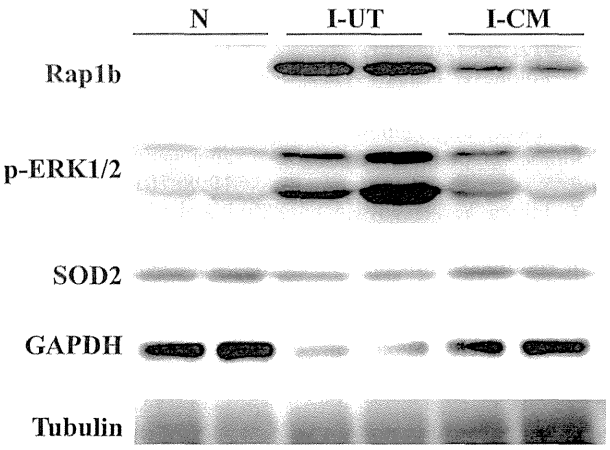

Supplemental Fig. 1.
A representative Western blot analysis of Rap1b, p-ERK1/2, SOD-2 GAPDH and Tubulin in ischemic muscle tissue specimens at 4 days after ischemia. Rap1b, Ras-associated protein 1B; pERK1/2, phospho-ERK1/2; SOD2, superoxide dismutase 2; GAPDH, glyceraldehyde-3-phosphate dehydrogenate; N, non-ischemic muscle; I-UT, ischemic muscle without treatment; I-CM, ischemic muscle with CO_2 mist treatment.

Heart Vessels
DOI 10.1007/s00380-015-0652-6

ORIGINAL ARTICLE

Characteristic patterns of the longitudinal and circumferential distribution of calcium deposits by parent coronary arteries observed from computed tomography angiography

Shoichi Ehara · Kenji Matsumoto · Takao Hasegawa · Kenichiro Otsuka · Mikumo Sakaguchi · Kenei Shimada · Junichi Yoshikawa · Minoru Yoshiyama

Received: 23 May 2014 / Accepted: 13 February 2015

Abstract Many investigators have reported that the total amount of coronary calcium correlates with the overall magnitude of atherosclerotic plaque burden in the entire coronary tree and is a powerful predictor of future cardiovascular events. However, the development and spatial distribution of coronary calcifications remain unclear. We investigated the spatial distribution of calcifications throughout the coronary tree during coronary artery evaluation using coronary computed tomography angiography (CTA). A further aim was to assess the progression of existing calcifications and the development of new deposits in a follow-up study. The study population consisted of 287 patients for the cross-sectional study using CTA to evaluate the spatial distribution of calcifications by parent coronary arteries. Next, we analyzed a CTA dataset of 57 patients who had undergone two CTA examinations. In this group, the two CTA images were used for assessing the progression of existing calcifications and the development of new deposits. The coronary calcifications tended to be clustered within the proximal and middle portions. Moreover, in the proximal left anterior descending coronary artery (LAD), small calcifications were located more toward the inner pericardial side. Finally, new calcium deposits developed within the proximal and middle portions of the LAD and left circumflex coronary artery, but those in the right coronary artery were likely to appear evenly from the proximal to the distal portion. This study shows the characteristic patterns of the longitudinal and circumferential distribution of calcifications by parent coronary arteries.

Keywords Calcium · Coronary artery · Computed tomography · Atherosclerosis

Abbreviations

CT	Computed tomography
IVUS	Intravascular ultrasound
CAD	Coronary artery disease
CTA	Computed tomography angiography
ECG	Electrocardiography
TCS	Total coronary calcium score
MPR	Multiplanar reconstruction
PWMIP	Partial width maximum intensity projection
LAD	Left anterior descending coronary artery
LCx	Left circumflex coronary artery
RCA	Right coronary artery
ACS	Acute coronary syndrome

Introduction

Atherosclerotic plaque calcification has usually been considered an indicator of long-standing advanced atherosclerotic disease. Several studies have focused on the mechanism and role of calcification in atherosclerotic plaque development. In particular, following the introduction of non-contrast electron-beam computed tomography (CT), many investigators have reported that the total amount of coronary calcium correlates with the overall magnitude of atherosclerotic plaque burden in the entire coronary tree [1–3], and is a powerful predictor of future cardiovascular

S. Ehara (✉) · K. Matsumoto · T. Hasegawa · K. Otsuka · M. Sakaguchi · K. Shimada · M. Yoshiyama
Department of Cardiovascular Medicine, Osaka City University Graduate School of Medicine, 1-4-3 Asahi-machi, Abeno-ku, Osaka 545-8585, Japan
e-mail: ehara@med.osaka-cu.ac.jp

J. Yoshikawa
Nishinomiya Watanabe Cardiovascular Center, Nishinomiya, Hyogo, Japan

Published online: 25 February 2015

events [4]. Identification and quantification of coronary calcium by non-contrast CT may well be one of the best non-invasive methods currently available to estimate the extent of coronary atherosclerotic plaque burden.

Previous pathological and intravascular ultrasound (IVUS) studies have shown that atherosclerotic plaques in patients with coronary artery disease (CAD) occur in the proximal portions of the major coronary arteries, and tend to be located along the inside of the vessel curve [5–8]. IVUS is the optimal technique to investigate the distribution of atherosclerotic plaques using direct visualization of plaque burden in the culprit vessel, but not throughout the coronary tree, including non-culprit vessels. Moreover, this modality is unsuitable for the observation of mildly stenotic lesions that have not yet caused cardiac ischemia in subjects without CAD.

Recently, coronary computed tomography angiography (CTA) has reached a spatial and temporal resolution high enough for assessment of not only coronary artery stenosis, but also atherosclerotic plaques [9]. However, the level of contrast enhancement in the coronary vessels may obscure plaque and may interfere with reliable measurements of plaque density, especially in non-calcified plaques [10]. Nevertheless, it is conceivable that owing to the relatively high density of calcified plaques compared with non-calcified plaques, the amount of coronary calcium deposits could be estimated by CTA. Only a few studies have addressed this issue previously [11, 12]. Here, we hypothesized that although coronary CTA is for evaluating coronary artery stenosis, it might allow us to assess the longitudinal and circumferential distribution patterns of calcium deposits within the entire coronary artery tree in much greater detail than non-contrast axial CT, even in patients who are suspected of having CAD but are found not to have significant coronary artery stenosis. To the best of our knowledge, there have been no previous CTA studies on the spatial distribution and progression patterns of calcium deposits by parent coronary arteries.

This study comprised 2 components. First, given the spatial distribution of calcium deposits by parent coronary arteries, we conducted a cross-sectional study. Second, we retrospectively analyzed a CTA dataset of patients who had undergone two CTA examinations to assess the progression of existing coronary calcium and the development of new deposits.

Patients and methods

Patients

First, we retrospectively analyzed CT data from 292 consecutive patients between May 2008 and March 2010 who were suspected of having CAD or who had at least one coronary risk factor and clinical indications for CTA for coronary artery evaluation (a cross-sectional study). Patients with atrial fibrillation, previous coronary artery bypass grafting, or percutaneous transluminal intervention were excluded from the study, because these factors affect coronary calcium deposits. Five of the 292 patients were excluded because the images were of insufficient quality for analysis of the distribution of coronary calcium deposits. Thus, the study population comprised 287 patients (mean age 64 years, range 33–88 years, 71 % men) for the cross-sectional study. In this group, imaging was used to evaluate the extent and spatial distribution of calcium deposits by parent coronary arteries.

Second, we analyzed the CT dataset of 57 patients (mean age 62 years, range 38–81 years, 74 % men), who had undergone two CTA examinations between May 2008 and March 2013 (a retrospective follow-up study). These patients were referred for a follow-up CTA examination on the basis of the physician's clinical judgment because at least one parent vessel with intermediate stenosis was present. In this group of patients who underwent follow-up examinations, two CTA images were used to assess the progression of existing coronary calcium deposits and the development of new deposits.

Informed consent was obtained from all patients, and the study was approved by the hospital ethics committee.

CT image acquisition

The patients were scanned in the supine position during a single breath-hold in the craniocaudal direction using a 64-slice CT scanner (SOMATOM Sensation 64 Siemens, Germany). Patients with a heart rate of >65 beats/min received 2.5 or 5 mg bisoprolol fumarate orally 2 h before the CTA scan. In addition, all patients received 0.6 mg nitroglycerin sublingually immediately before scanning. The electrocardiographic (ECG) signal was digitally recorded during the scan and all patients included showed sinus rhythm throughout the scan.

First, to determine the calcium score, a non-contrast ECG gated scan was performed using standardized parameters (tube voltage of 120 kV, an effective tube current–time product of 100 effective mAs, collimation of 24 × 1.2 mm, and gantry rotation time of 330 ms). Then, for CTA, 50–85 mL of contrast medium (Iopamiron 370; Bayer HealthCare, Berlin, Germany) was injected through a dual-head injector at a rate of 2.5–5.0 mL/s (body weight × 0.06 mL/s/kg) into a cubital vein, followed by 30 mL of saline solution chaser. A bolus tracking technique was used to synchronize the arrival of the contrast in the coronary arteries, and the scan was started once contrast attenuation in a preselected region of interest

in the ascending aorta reached a predefined threshold of +150 Hounsfield units (HU). CTA examination was performed with a tube voltage of 120 kV, an effective tube current–time product of 770 effective mAs, a collimation of 64 × 0.6 mm, a pitch of 0.2, and a gantry rotation time of 330 ms.

CT image reconstruction

First, non-contrast images for the measurement of coronary calcium scores were obtained with a slice thickness of 3 mm, with slices starting at the level of the carina and proceeding to the level of the diaphragm. Tomographic imaging was electrocardiographically triggered to 60–80 % of the R–R interval. Coronary calcification was defined as a volume of 2 consecutive pixels with a CT number of >130 HU within the distribution of a coronary artery. All sections of the CT scan obtained were then reviewed by an experienced investigator who was blinded to all clinical data. The intraobserver correlation was 0.99. The quantitative coronary calcium score was calculated according to the method described by Agatston et al. [13]. The total coronary calcium score (TCS) was defined as the sum of the scores for each lesion. Four absolute TCS categories were considered: zero score (TCS = 0), mild score (0 < TCS < 100), moderate score (100 ≤ TCS < 400), and severe score (TCS ≥ 400).

Then, to obtain nearly motion-free image quality, axial image series of the contrast-enhanced CTA datasets were reconstructed within the mid- to end-diastolic phase, using retrospective ECG gating. The first heart phase reconstruction was performed at 70 % of the R–R interval. Additional reconstructions in 5 % steps were performed if motion artifacts were present. Datasets with the least artifacts in a single coronary vessel were selected and sent to a dedicated workstation (Virtual Place; AZE, Tokyo, Japan), where subsequent evaluation was conducted with 0.75-mm effective slice thickness and 0.4-mm increment. A field of view of 180 × 180 mm^2, a 512 × 512 matrix, and a medium smooth convolution kernel (B25f) were applied.

Evaluation of extent and distribution of calcium deposits

Calcium deposits within all coronary artery segments >2 mm in diameter were evaluated using curved multiplanar reconstruction (MPR) and partial width maximum intensity projection (PWMIP) images generated by Virtual Place visualization software (AZE, Tokyo, Japan). Briefly, the software extracts the centerline of coronary arteries and calculates radial basis function by coronary centerline. It makes a smooth flat surface area from the curve line through all coronary on all axial images. Then, the software adds surface thickness, which is calculated as maximum intensity projection and displayed on the viewer. Any structure on the vessel wall with a CT density above that of the contrast-enhanced coronary lumen was identified as a calcium deposit. If a possible calcium deposit was visually unclear or difficult to distinguish (CT density below that of the contrast-enhanced coronary lumen), its location was marked, and the identification was confirmed with non-contrast imaging. The area to be imaged using non-contrast axial CT was carefully matched to the corresponding marked area in the contrast axial image according to the surrounding cardiac and chest wall structures. In addition, any structure on the coronary artery wall with a CT density of >130 HU in a non-contrast image was identified as a calcium deposit (Fig. 1) [14].

For the first cross-sectional study, the size of calcium deposits in the proximal, middle, and distal coronary segments of the left anterior descending coronary artery (LAD), left circumflex coronary artery (LCx), right coronary artery (RCA), large side branches, and left main artery was assessed according to the modified classification of the American Heart Association [15, 16]. The proximal LAD was defined as the arterial region from the left main bifurcation to the first major septal branch. The vessel segment from the first major septal branch to the apex of the heart was divided in half, with the middle LAD comprising the partial segment closest to the branch and the distal LAD comprising the partial segment closest to the apex. The proximal LCx was defined as the main stem of the LCx from its origin off left main bifurcation to the obtuse marginal branch. The middle LCx was defined as the stem of the LCx distal to the origin of the obtuse marginal branch and running along or close to the posterior left atrioventricular groove. The vessel segment from the ostium to the acute margin of the heart was divided in half, with the proximal RCA comprising the partial segment closest to the ostium and the middle RCA comprising the partial segment closest to the heart margin. The distal RCA was defined as the region from the acute margin to the origin of the posterior descending branch. On the basis of the size of each coronary calcium deposit, each segment was classified into one of 4 groups: a no calcification segment was defined as one in which calcium was not detected, a small calcification segment was defined as one in which a calcium deposit <3 mm of longitudinal length on MPR images and occupying only 1 side on cross-sectional images was present, an intermediate calcification segment was defined as one in which a calcium deposit with a length of 3–8 mm and/or occupying more than 1 side on cross-sectional images was present, and a large calcification segment was defined as one in which the calcification was larger than 8 mm in size [17, 18]. In each segment, the largest size of the calcium deposit obtained was assigned per coronary segment and was used for final analysis.

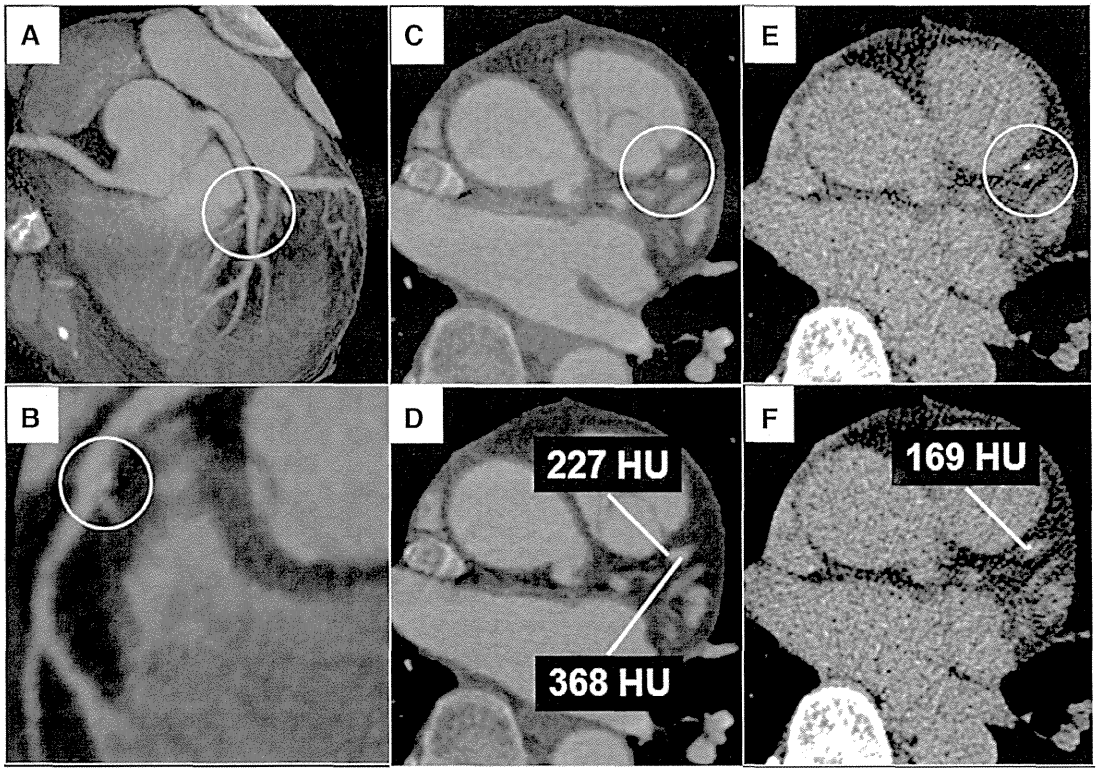

Fig. 1 Identification of the calcium deposit with low HUs. **a–d** Displays contrast-enhanced CTA images showing an area of potential calcium deposition. Deposition was unclear or difficult to distinguish because the structure had a CT density below that of the contrast-enhanced coronary lumen. **e** and **f**, Calcium was ascertained as a structure with a CT density of >130 HU that could be assigned to the coronary artery wall in a non-contrast image

When a segment was classified as "small calcification segment" in the parent vessels of the LAD, LCx, and RCA, the circumferential distribution of the calcium deposit within the vessel wall at that segment was visually assessed with regard to following 2 points, referred to the previous report [19]: (A) the side of the pericardium or myocardium on the curved MPR images and (B) the side of the atrium or ventricle for parent vessels of the RCA and LCx and the inner (right ventricle) or lateral side for the LAD on the PWMIP images (Fig. 2). In cases where a small calcium deposit (<3 mm in length) was present on more than 1 side, the side with the center of the calcium deposit was chosen for grouping. Calcium distribution was recorded as "unclassified" when such a small calcium deposit occupied the entire lumen because of small vessel diameter or when the center of the small calcium deposit was just on the center of the vessel. On the basis of this information, the circumferential distribution of small calcifications was divided into 8 directions (Fig. 3). In both "intermediate calcification" and "large calcification" segments, it was not possible to reliably assess the circumferential distribution of calcium deposits because of the extent of the calcium deposit. Consequently, the circumferential distribution in these segments was not assessed.

The CT image dataset was analyzed by 2 experienced cardiologists who were blinded to the clinical data. In case of disagreement, consensus was reached by an additional joint reading. The κ values for inter- and intra-observer agreements with regard to classification according to the calcium deposit size were 0.89 and 0.93, respectively, whereas κ values with regard to classification of the calcium circumferential distribution into 8 directions were 0.89 and 0.92, respectively.

Progression of existing calcium deposits and development of new deposits: serial follow-up data

We retrospectively analyzed the CT dataset of 57 patients who had undergone two CTA examinations to assess the progression of existing coronary calcium deposits and the development of new deposits. First, the size and longitudinal distribution of all calcium deposits were recorded from baseline images. Then, for follow-up images, progression in the size of previous calcium deposits and the development of new calcium deposits were observed. When the size of each calcium deposit was classified into categories for larger deposits on follow-up images, compared

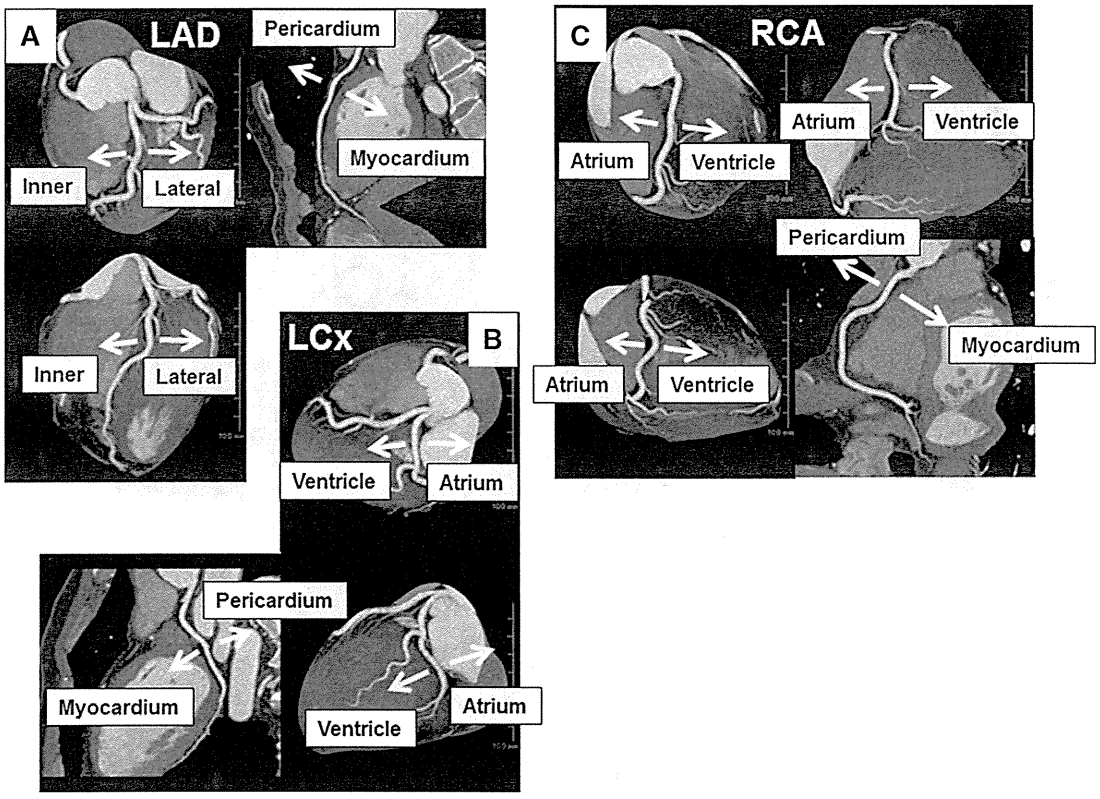

Fig. 2 Circumferential distribution of small calcium deposits. **a** Small calcium deposits were detected on the inner (right ventricle) or lateral side on the PWMIP images and on the side of the pericardium or myocardium on the curved MPR images for the LAD. **b** and **c** Small calcium deposits were detected on the side of the atrium or ventricle on the PWMIP images and on the side of the pericardium or myocardium on the curved MPR images for parent vessels of the RCA and LCx

with the category on baseline images, that calcium deposit was described as having progressed in size. On the basis of the change in size or the development of new coronary calcium deposits between 2 CT examinations, each patient was classified into one of 4 groups: the no change group included patients in whom calcium deposits did not change in size or number; the progression group included patients in whom any calcium deposit became larger but the number of deposits did not change; the new development group included patients in whom at least 1 new calcium deposit appeared; the progression and new development group included patients in whom any calcium deposit became larger and at least 1 new calcium deposit appeared.

Statistical analysis

The results are expressed as mean ± SD. Statistical comparisons between more than 3 groups were performed using one-way analysis of variance and post hoc multiple comparison using Scheffe's test. Categorical variables were compared using the Chi square test. All calculations were performed using JMP software (version 10, SAS Institute Inc., Cary, North Carolina, USA) and values of $p < 0.05$ were considered significant.

Results

Extent of calcium deposits

The clinical characteristics of all 287 patients are shown in Table 1. The 287 patients included 101 patients (35 %) with a zero TCS. In the remaining 186 (65 %) patients, 82 patients (29 %) had a mild TCS, 53 (18 %) had a moderate TCS, and 51 (18 %) had a severe TCS. Overall, calcium deposits were observed in 804 (29 %) of 2777 segments in 186 patients with mild, moderate, and severe TCS. As shown in Fig. 4a, the frequency of segments with calcium deposits for all segments was significantly different among the mild, moderate, and severe TCS groups ($p < 0.0001$). Calcium deposits were observed in 170 (14 %) of 1225 segments in 82 patients with a mild TCS, 213 (27 %) of 782 segments in 53 patients with a moderate TCS, and in 421 (55 %) of 770 segments in 51 patients with a severe TCS.

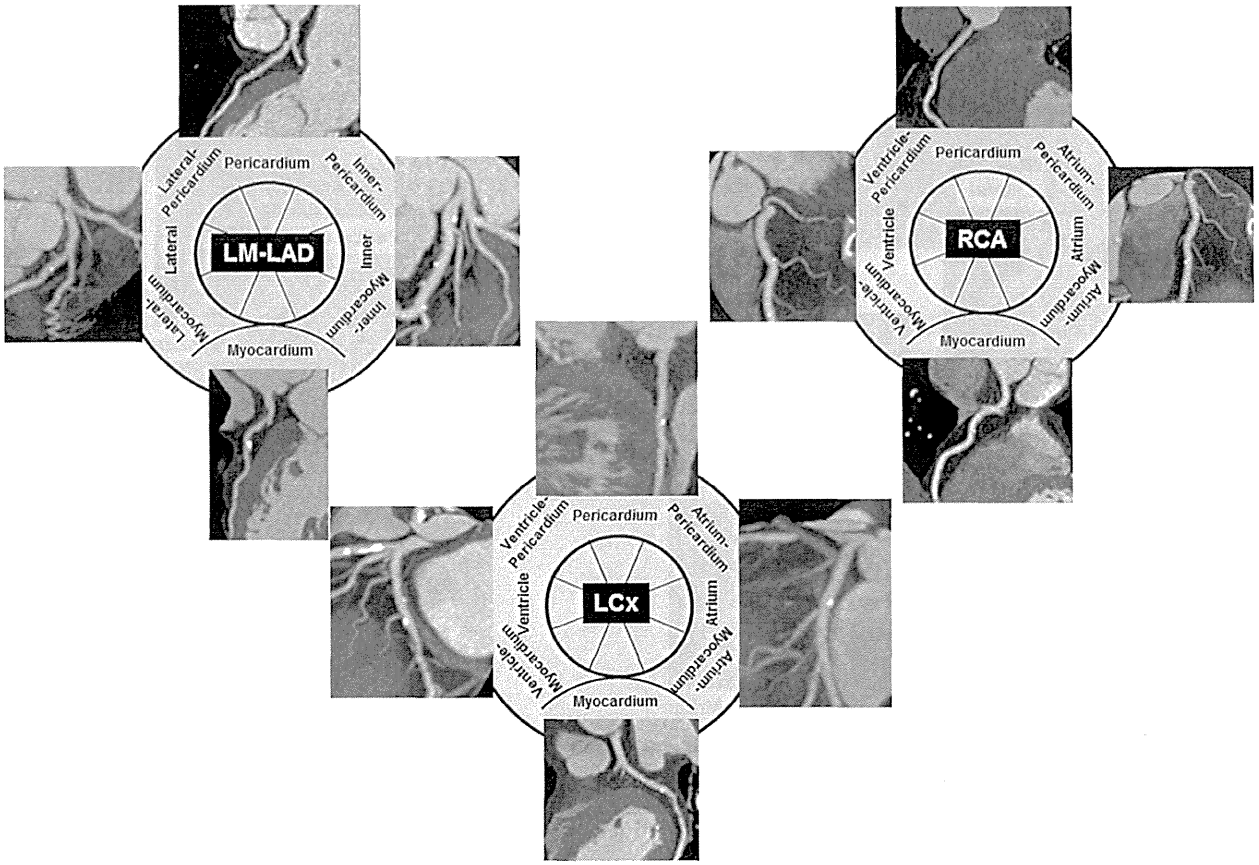

Fig. 3 Eight directions of the circumferential distribution of small calcifications

Table 1 Patient characteristics

	Value
Total number	287
Age, (years)	64 ± 11 (range 33–88)
Male, *n* (%)	203 (71)
Hypertension, *n* (%)	183 (64)
Diabetes mellitus, *n* (%)	68 (24)
Hypercholesterolemia, *n* (%)	135 (47)
Smoker, *n* (%)	118 (41)
Body mass index (kg/m^2)	24.0 ± 4.4
Blood pressure	
Systole (mm Hg)	135 ± 19
Diastole (mm Hg)	84 ± 12
Heart rate during scanning (beats/min)	62 ± 10
Total coronary calcium score	
Zero	101 (35)
Mild	82 (29)
Moderate	53 (18)
Severe	51 (18)
Coronary artery stenoses with a lumen reduction of >50 % detected by CTA	40 (14)

Values are mean ± standard deviation or *n* (percentage)

CTA computed tomography angiography

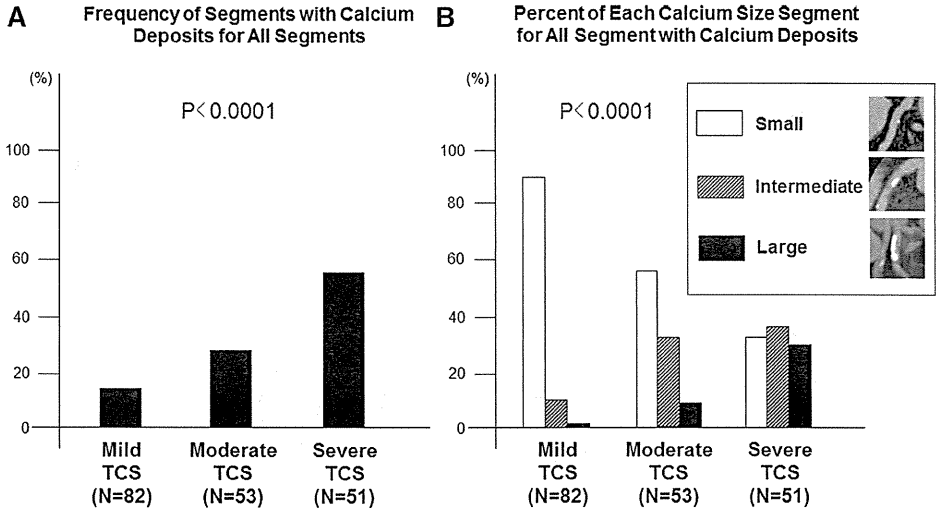

Fig. 4 Characteristics of calcium deposits in patients with a mild, moderate, and severe TCS. **a** The frequency of segments with calcium deposits for all segments. **b** The frequency of each type of segment with regard to the size of the calcium deposit (small, intermediate, or large) for all segments with calcium deposits. *Open bar* small calcification segment. *Striped bar* intermediate calcification segment. *Solid bar* large calcification segment

Four hundred and eleven (51 %) of 804 segments containing calcium deposits were classified as small calcification segments, 246 (31 %) as intermediate, and 147 (18 %) as large. As shown in Fig. 4b, the frequency of each segment type according to the size of the calcium deposit (small, intermediate, or large) for all segments with calcium deposits was also significantly different among the 3 TCS groups ($p < 0.0001$). The frequency of small calcification segments for all segments with calcium deposits was the highest in the mild TCS group, whereas the frequency of type of segment with regard to the size of the calcium deposit in the severe TCS group was relatively even from small to large calcium deposits.

Distribution of calcium deposits

Figure 5 shows the longitudinal distribution of 804 segments containing calcium deposits of any size among the LAD, LCx and RCA in detail. The calcium deposits were primarily located in the proximal and middle segments of the LAD and LCx and were uncommon in the distal segment. In the RCA, the calcium deposits were observed primarily in the proximal and middle segments, but the distal segment contained more calcium deposits than the distal segment of the LAD or the posterolateral left ventricular branch of the LCx.

Figure 6 shows the circumferential distribution of the small calcium deposits ($n = 324$) at each segment in the parent vessels of the LAD, LCx, and RCA. In the proximal and middle segments of the LAD including the left main artery, small calcium deposits were oriented more toward the inner pericardial side than the myocardial or lateral side. Only 10 LADs had small calcium deposits in their distal segments. Among these deposits, distribution was recorded as "unclassified" in 6 cases because the

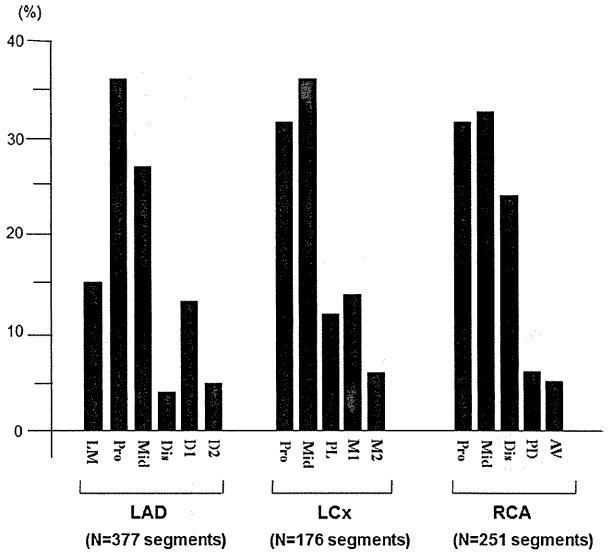

Fig. 5 The longitudinal distribution of 804 segments containing calcium deposits of any size among the LAD, LCx and RCA. *LAD* left anterior descending coronary artery, *LCx* left circumflex coronary artery, *RCA* right coronary artery, *LM* left main artery, *D* diagonal branch, *PL* posterolateral left ventricular branch, *M* obtuse marginal branch, *PD* posterior descending branch, *AV* atrioventricular branch, *Pro* proximal, *Mid* middle, *Dis* distal

deposit occupied the entire lumen. Small calcifications in the proximal segment of the LCx tended to be located more toward the atrial side than the ventricular side, and those in the middle portion of the LCx were present more frequently toward the myocardial–ventricular side. Small calcium deposits from the proximal to the distal segments of the RCA were located more toward the myocardial and/or ventricular side, but there was no definite tendency.

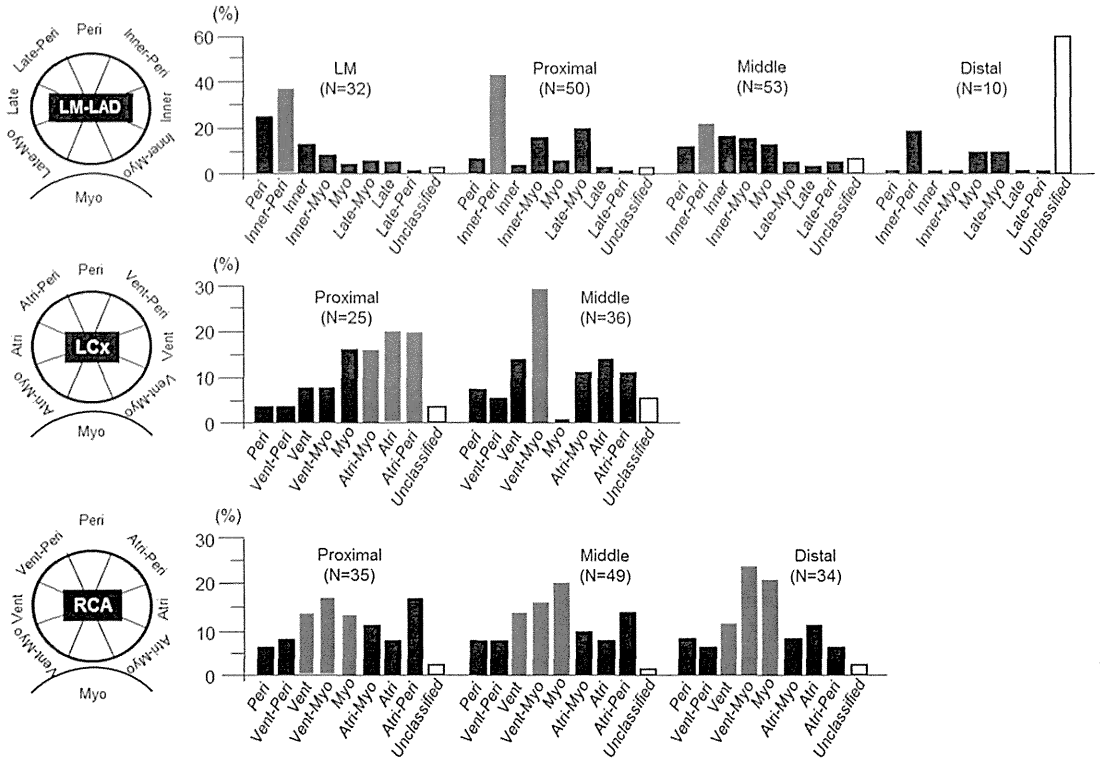

Fig. 6 The circumferential distribution of small calcium deposits according to the vessels. *Peri* pericardial side, *Myo* myocardial side, *Late* lateral side, *Vent* ventricular side, *Atri* atrial side

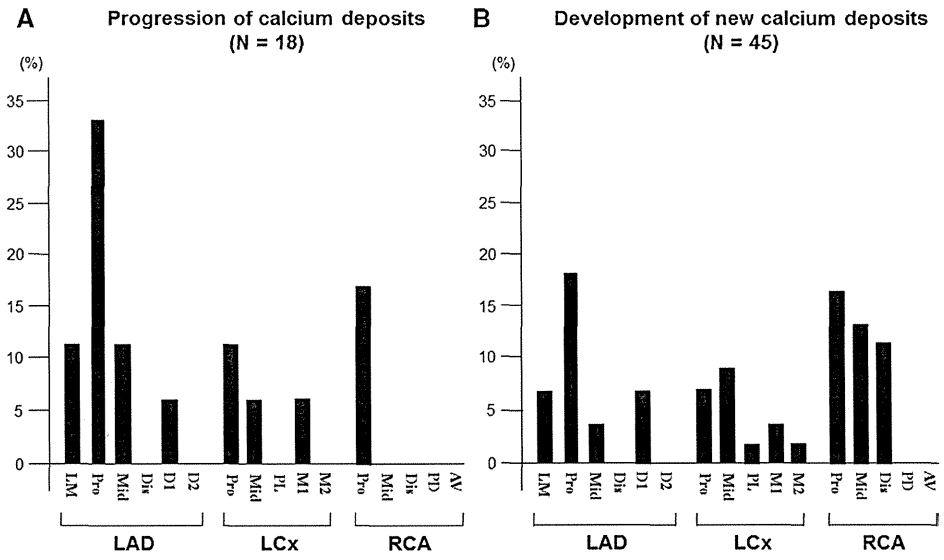

Fig. 7 The longitudinal distribution of the progression of calcium deposits (**a**) and development of new calcium deposits (**b**) during the follow-up period. For abbreviations see Fig. 5

Follow-up study for calcium deposits

Sixteen (28 %) of 57 patients who underwent 2 CT examinations had no coronary calcium deposits during the study period (mean follow-up period, 22 ± 14 months). In the remaining 41 (72 %) patients (mean follow-up period, 21 ± 11 months), 18 patients (31 %) were assigned to the no change group, 3 (5 %) to the progression group, 14 (24 %) to the new development group, and 6 (10 %) to the progression and new development group. Eighteen calcium deposits increased in size, and 45 new calcium deposits developed during the study period. Figure 7 shows

the longitudinal distribution of the progression of calcium deposits and development of new calcium deposits during the follow-up period. Calcium deposits that showed progression in size tended to be clustered within the proximal portion of the parent vessels. Conversely, the development of new coronary calcium deposits occurred within the proximal and middle portions in the LAD and LCx, but those in the RCA were likely to appear evenly from the proximal to the distal portion.

Discussion

Even during the CTA, we found the characteristic distribution patterns of calcium deposits by parent coronary arteries. First, coronary calcium deposits were not uniformly distributed throughout the coronary tree but tended to be clustered within the proximal and middle portions, except in the case of the RCA. Second, there was a characteristic pattern of circumferential distribution of small calcium deposits according to the parent coronary arteries. Finally, this is the first study to demonstrate that calcium deposits that showed progression in size tended to be clustered within the proximal portion of the parent vessels and the development of new coronary calcium deposits also occurs within the proximal and middle portions of the LAD and LCx, but those in the RCA are likely to appear evenly from the proximal to distal portion.

Several investigators have noted the longitudinal spatial distribution of atherosclerotic plaques throughout the coronary tree using IVUS or CT [8, 16, 20]. Many studies have reported that coronary plaques are frequently located in the proximal and middle segments of the major coronary arteries. Overall, our present data, based on both quantitative and qualitative analysis of calcium deposits, are in agreement with these previous findings, although the pattern of the circumferential spatial distribution of atherosclerotic plaques within the vessel wall was not investigated in the previous studies. The total amount of coronary calcification correlates with the overall magnitude of atherosclerotic plaque burden in the entire coronary tree [1–3]. However, few clinicians consider the TCS to be a good discriminator of significant stenosis, because the specificity for detection of significant stenosis is relatively low. The location and amount of calcification are reported to be positively, but nonlinearly, associated with narrowing of the lumen of coronary vessels [3, 21, 22]. Kajinami et al. [23] compared, on a site by site basis, the morphologic features of coronary calcifications determined by electron-beam CT and coronary atherosclerosis determined by coronary angiography, and reported that the calcification morphology was associated with significant stenosis and angiographic lesion morphology. Thus, the distribution and development of calcium deposits may influence the progression of atherosclerotic plaques and plaque morphology.

Regarding the circumferential spatial distribution of atherosclerotic plaques, some IVUS studies have demonstrated that coronary atherosclerotic plaques in the very proximal LAD portion are localized on the wall opposite to the LCx takeoff and form preferentially along the inner arc of the coronary vessel [5, 6, 8]. However, these studies examined atherosclerotic plaques only in the very proximal segment of the LAD and, therefore, complete proximal, middle, and distal segments of the whole coronary tree including non-culprit vessels could not be analyzed. Preferential sites of atherosclerosis are normally branching or curved arteries, where blood flow is non-linear and slow, which exerts pro-atherogenic low, or oscillatory shear stress [24]. Low shear stress occurs in inner curvatures, such as opposite the LCx and myocardial aspect of LAD. Oscillatory shear stress involves changes in both the magnitude of shear stress and direction of blood flow, normally at branch points, bifurcations or downstream of stenosis [25]. However, due to the asymmetrical and complex structure of bifurcations and bends in the coronary artery, the exact flow patterns were highly asymmetrical and far more complex than those observed in model vessels. Therefore, these findings cannot be generalized across all cases encountered in the human coronary tree, nor used to describe the detailed characteristics of flow at each location on the arterial tree [7, 26]. Clearly, among the 3 major coronary arteries, there are differences in blood flow patterns, flow separation (side branches), and flow turbulence, which result in different wall shear stresses. As shown in the present study, it is very interesting that there was a different pattern of the circumferential distribution of small calcium deposits by parent coronary arteries.

The clinical relevance and role of calcification in plaque vulnerability in patients with acute coronary syndrome (ACS) is still controversial. Our previous quantitative and qualitative IVUS analysis of calcifications demonstrated that the culprit segments of patients with ACS were mostly characterized by the presence of spotty calcification, associated with fibrofatty plaques and positive remodeling [27]. In this study population, no one suffered from ACS and any plaque morphology except for the coronary calcium deposits was not assessed. We propose that the term "spotty calcification" be used to represent the small and discrete calcium deposits associated with fibrofatty plaques and positive remodeling in patients with ACS. In general, calcification itself is considered to be part of the process of atherosclerosis, but its process is different from the acute progression following plaque rupture. Therefore, we used the term "small calcification" on the basis of the size of each coronary calcium deposit in the present study.

The understanding of natural history of atherosclerotic plaque development will ultimately require serial

observation of mildly atherosclerotic lesions that have not yet caused an acute coronary event or induced cardiac ischemia, using non-invasive modalities such as CT or magnetic resonance imaging [28]. Thus far, several studies have attempted to validate the use of CTA for measuring coronary calcium score to obviate the need for a separate non-contrast CT scan and decrease radiation dose [11, 12]. However, there have been no previous CTA studies on the spatial distribution and progression patterns of coronary calcium deposits. This CTA study, although CTA is for evaluating coronary artery stenosis, demonstrates that calcium deposits that show progression in size tend to be clustered within the proximal portion of the vessel, especially in the LAD. The relationship of the proximal LAD stenosis to sudden cardiac death has been confirmed in a general population [29]. Our results suggest that during checking for calcium deposits, particular attention should be paid to the proximal portion of the LAD. The findings of our retrospective follow-up study may seem merely to reiterate commonly accepted results from studies with other modalities instead of being of obvious significance or providing new information to improve patient care. Nevertheless, we believe that our attempt to test the conventional wisdom by retrospective analysis of routinely acquired CTA data obtained to check for coronary artery stenosis is important for educational and scientific purposes.

This study has a number of limitations. First, the biggest limitation of this study is that CTA is used to assess the coronary calcium deposits. The relatively high radiation dose and use of iodinated contrast material required by CTA should be emphasized. For these reasons, we cannot presently adopt coronary CTA as the primary method of analyzing the distribution patterns of coronary calcium deposits. Second, in this study non-calcified and mixed plaques were not assessed. CTA has the capacity to provide additional information on non-calcified and mixed plaques rather than calcified [14, 18–20]. Combining the analysis of coronary anatomy, stenosis and these complex plaques may provide incremental value into this study. Third, all analyses for the first, cross-sectional study were not per lesion but per segment, although per lesion analyses were performed for the second, retrospective follow-up study. When small and large calcium deposits existed in the same segment, the distribution of the large calcium deposit was recorded and the small one was not analyzed. We chose "per segment" analyses in the cross-sectional study because the presence of large calcium deposits can sometimes conglutinate other calcium deposits, which causes difficulty in distinction and subsequent interpretation of the data. However, this method of analysis could have masked important findings and potentially led to inaccuracies. Further studies, using "per lesion" analyses, are needed to assess more detailed distribution, progression, and development patterns of calcified and non-calcified plaques by parent coronary arteries. Fourth, the number of patients with serial follow-up data was relatively small. Essentially, our present study cohort based on physicians' clinical judgment was not designed to assess the formation of calcium deposits. Fifth, to our regret, we did not assess the effects of medication on coronary artery calcium development and progression. However, the aim of this study is to investigate the spatial distribution of coronary calcium deposits, and their progression and the development pattern, not to assess the factors associated with these phenomena. Finally, our cohort did not include patients with ACS who may have a different spatial distribution of calcium deposits.

In conclusion, this study shows the characteristic patterns of the longitudinal and circumferential distribution of calcium deposits by parent coronary arteries. This is the first study to determine that calcium deposits that show progression in size tend to be clustered within the proximal portion of the vessel, especially in the LAD. Thus, we should pay particular attention to the proximal portion of the vessel when checking patients for calcium deposits.

Conflict of interest The authors declare that there are no financial or other relations that could lead to a conflict of interest.

References

1. Simons DB, Schwartz RS, Edwards WD, Sheedy PF, Breen JF, Rumberger JA (1992) Noninvasive definition of anatomic coronary artery disease by ultrafast computed tomographic scanning: a quantitative pathologic comparison study. J Am Coll Cardiol 20:1118–1126
2. Rumberger JA, Simons DB, Fitzpatrick LA, Sheedy PF, Schwartz RS (1995) Coronary artery calcium area by electron-beam computed tomography and coronary atherosclerotic plaque area. A histopathologic correlative study. Circulation 92:2157–2162
3. Sangiorgi G, Rumberger JA, Severson A, Edwards WD, Gregoire J, Fitzpatrick LA, Schwartz RS (1998) Arterial calcification and not lumen stenosis is highly correlated with atherosclerotic plaque burden in humans: a histologic study of 723 coronary artery segments using nondecalcifying methodology. J Am Coll Cardiol 31:126–133
4. Keelan PC, Bielak LF, Ashai K, Jamjoum LS, Denktas AE, Rumberger JA, Sheedy PF II, Peyser PA, Schwartz RS (2001) Long-term prognostic value of coronary calcification detected by electron-beam computed tomography in patients undergoing coronary angiography. Circulation 104:412–417
5. Kimura BJ, Russo RJ, Bhargava V, McDaniel MB, Peterson KL, DeMaria AN (1996) Atheroma morphology and distribution in proximal left descending coronary artery: in vivo observations. J Am Coll Cardiol 27:825–831
6. Watanabe H, Yoshida K, Akasaka T, Hozumi T, Yoshikawa J (1996) Intravascular ultrasound assessment of plaque distribution in the ostium of the left anterior descending coronary artery. Am J Cardiol 78:827–829
7. Badak O, Schoenhagen P, Tsunoda T, Magyar WA, Coughlin J, Kapadia S, Nissen SE, Tuzcu EM (2003) Characteristics of atherosclerotic plaque distribution in coronary artery bifurcations: an intravascular ultrasound analysis. Coron Artery Dis 14:309–316

8. Iwami T, Fujii T, Miura T, Otani N, Iida H, Kawamura A, Yoshitake S, Kohno M, Hisamatsu Y, Iwamoto H, Matsuzaki M (1998) Importance of left anterior descending coronary artery curvature in determining cross-sectional plaque distribution assessed by intravascular ultrasound. Am J Cardiol 82:381–384
9. Fujimura T, Miura T, Nao T, Yoshimura M, Nakashima Y, Okada M, Okamura T, Yamada J, Ohshita C, Wada Y, Matsunaga N, Matsuzaki M, Yano M (2014) Dual-source computed tomography coronary angiography in patients with high heart rate. Heart Vessels 29:443–448
10. Cademartiri F, Mollet NR, Runza G, Bruining N, Hamers R, Somers P, Knaapen M, Verheye S, Midiri M, Krestin GP, de Feyter PJ (2005) Influence of intracoronary attenuation on coronary plaque measurements using multislice computed tomography: observations in an ex vivo model of coronary computed tomography angiography. Eur Radiol 15:1426–1431
11. van der Bijl N, Joemai RM, Geleijns J, Bax JJ, Schuijf JD, de Roos A, Kroft LJ (2010) Assessment of Agatston coronary artery calcium score using contrast-enhance CT coronary angiography. Am J Roentgenol 195:1299–1305
12. Otton JM, Lønborg JT, Boshell D, Feneley M, Hayen A, Sammel N, Sesel K, Bester L, McCrohon J (2012) A method for coronary artery calcium scoring using contrast-enhanced computed tomography. J Cardiovasc Comput Tomogr 6:37–44
13. Agatston AS, Janowitz WR, Hildner FJ, Zusmer NR, Viamonte M Jr, Detrano R (1990) Quantification of coronary artery calcium using ultrafast computed tomography. J Am Coll Cardiol 15:827–832
14. Kitagawa T, Yamamoto H, Ohhashi N, Okimoto T, Horiguchi J, Hirai N, Ito K, Kohno N (2007) Comprehensive evaluation of noncalcified coronary plaque characteristics detected using 64-slice computed tomography in patients with proven or suspected coronary artery disease. Am Heart J 154:1191–1198
15. Austen WG, Edwards JE, Frye RL, Gensini GG, Gott VL, Griffith LS, McGoon DC, Murphy ML, Roe BB (1975) A reporting system on patients evaluated for coronary artery disease. Report of the Ad Hoc Committee for Grading of Coronary Artery Disease, Council on Cardiovascular Surgery, American Heart Association. Circulation 51:5–40
16. Mollet NR, Cademartiri F, Nieman K, Saia F, Lemos PA, McFadden EP, Serruys PW, Krestin GP, de Feyter PJ (2005) Noninvasive assessment of coronary plaque burden using multislice computed tomography. Am J Cardiol 95:1165–1169
17. Ehara S, Kobayashi Y, Kataoka T, Yoshiyama M, Ueda M, Yoshikawa J (2007) Quantification of coronary calcification by intravascular ultrasound. Circ J 71:530–535
18. Motoyama S, Sarai M, Harigaya H, Anno H, Inoue K, Hara T, Naruse H, Ishii J, Hishida H, Wong ND, Virmani R, Kondo T, Ozaki Y, Narula J (2009) Computed tomographic angiography characteristics of atherosclerotic plaques subsequently resulting in acute coronary syndrome. J Am Coll Cardiol 54:49–57
19. van der Giessen AG, Wentzel JJ, Meijboom WB, Mollet NR, van der Steen AF, van de Vosse FN, de Feyter PJ, Gijsen FJ (2009) Plaque and shear stress distribution in human coronary bifurcations: a multislice computed tomography study. Eurointervention 4:654–661
20. Kashiwagi M, Tanaka A, Shimada K, Kitabata H, Komukai K, Nishiguchi T, Ozaki Y, Tanimoto T, Kubo T, Hirata K, Mizukoshi M, Akasaka T (2013) Distribution, frequency and clinical implications of napkin-ring sign assessed by multidetector computed tomography. J Cardiol 61:399–403
21. Haberl R, Becker A, Leber A, Knez A, Becker C, Lang C, Brüning R, Reiser M, Steinbeck G (2001) Correlation of coronary calcification and angiographically documented stenoses in patients with suspected coronary artery disease: results of 1764 patients. J Am Coll Cardiol 37:451–457
22. Ho JS, Fitzgerald SJ, Stolfus LL, Wade WA, Reinhardt DB, Barlow CE, Cannaday JJ (2008) Relation of a coronary artery calcium score higher than 400 to coronary stenoses detected using multidetector computed tomography and to traditional cardiovascular risk factors. Am J Cardiol 101:1444–1447
23. Kajinami K, Seki H, Takekoshi N, Mabuchi H (1997) Coronary calcification and coronary atherosclerosis: site by site comparative morphologic study of electron beam computed tomography and coronary angiography. J Am Coll Cardiol 29:1549–1556
24. Caro CG, Fitz-Gerald JM, Schroter RC (1971) Atheroma and arterial wall shear. Observation, correlation and proposal of a shear dependent mass transfer mechanism for atherogenesis. Proc R Soc Lond B Biol Sci 177:109–159
25. Giannoglou GD, Antoniadis AP, Koskinas KC, Chatzizisis YS (2010) Flow and atherosclerosis in coronary bifurcations. EuroInterv Suppl 6:16–23
26. Asakura T, Karino T (1990) Flow patterns and spatial distribution of atherosclerotic lesions in human coronary arteries. Circ Res 66:1045–1066
27. Ehara S, Kobayashi Y, Yoshiyama M, Shimada K, Shimada Y, Fukuda D, Nakamura Y, Yamashita H, Yamagishi H, Takeuchi K, Naruko T, Haze K, Becker AE, Yoshikawa J, Ueda M (2004) Spotty calcification typifies the culprit plaque in patients with acute myocardial infarction. An intravascular ultrasound study. Circulation 110:3424–3429
28. Ehara S, Nakamura Y, Matsumoto K, Hasegawa T, Shimada K, Takagi M, Hanatani A, Izumi Y, Terashima M, Yoshiyama M (2013) Effects of intravenous atrial natriuretic peptide and nitroglycerin on coronary vasodilation and flow velocity determined using 3 T magnetic resonance imaging in patients with nonischemic heart failure. Heart Vessels 28:596–605
29. Vlay SC, Burger L, Vlay LC, Yen O, Novotny H, Grimson R (1993) Prediction of sudden cardiac arrest: risk stratification by anatomic substrate. An Heart J 126:807–815